CHEMICAL ENGINEERING TRANSACTIONS
VOL. 81, 2020
A publication of AIDIC
The Italian Association of Chemical Engineering
Online at www.cetjournal.it
Guest Editors: Petar S. Varbanov, Qiuwang Wang, Min Zeng, Panos Seferlis, Ting Ma, Jiří J. Klemeš

**ISBN** 978-88-95608-79-2; **ISSN** 2283-9216
DOI: 10.3303/CET2081070

# Simulation of Carbon Capture from Flue Gas of a Coal-fired Power Plant by a Three-bed Pressure Swing Adsorption Process

Chu-Yun Cheng[a], Chia-Chen Kuo[a], Ming-Wei Yang[b], Zong-Yu Zhuang[b], Po-Wei Lin[a], Hong-Sung Yang[c], Cheng-Tung Chou[a,*]

[a]Department of Chemical and Materials Engineering, National Central University, Zhongli District, Taoyuan City, Taiwan
[b]Chemistry and Environment Laboratory, Taiwan Power Research Institute, Shulin District, New Taipei City, Taiwan
[c]Department of Applied Cosmetology, Hwa Hsia University of Technology, Zhonghe District, New Taipei City, Taiwan
t310030@ncu.edu.tw

In order to reduce carbon dioxide emissions, pressure swing adsorption (PSA) process was studied to capture carbon dioxide from flue gas in a coal-fired power plant. Pressure swing adsorption features its low energy consumption, low investment, and simple operation. This study aims to capture carbon dioxide from flue gas by PSA process for at least 85 % $CO_2$ purity and with the other stream of more than 90 % $N_2$ purity. To validate the accuracy of the PSA simulation program, the extended Langmuir-Freundlich equation was adopted to fit measured equilibrium data to describe the adsorption equilibrium of adsorbent zeolite 13X. Next, the simulation study used the linear driving force model and compared the results of breakthrough curves and desorption curves between experiments and simulation to verify the accuracy of the mass transfer coefficient $k_{LDF}$ value in linear driving force model. The agreement between experimental data and the simulation results is good. Further, the simulation was verified with the 100-hour cyclic-steady-state experiment of the 3-bed 9-step PSA process studied. Flue gas after desulphurisation and water removal (13.5 % $CO_2$, 86.5 % $N_2$) of subcritical 1 kW coal-fired power plant was taken as feed to the designed 3-bed 9-step PSA process. To find the optimal operating conditions, the central composite design (CCD) was used. After analysis, optimal operating conditions were obtained to produce a bottom product at 89.20 % $CO_2$ purity with 88.20 % recovery, and a top product at 98.49 % $N_2$ purity with 93.56 % recovery. The mechanical energy consumption was estimated to be 1.17 – 1.41 GJ/t-$CO_2$.

## 1. Introduction

According to the Global Carbon Budget climate report published by nearly 80 scientists (Le Quéré et al., 2018), the concerns of global carbon emission trends are pointed out, which show that slowing down carbon dioxide increase is urgent. There are three ways to capture carbon dioxide from power plants: post-combustion capture, pre-combustion capture, and oxyfuel combustion capture. The post-combustion capture technology is important due to its small impact on the industrial combustion process, so it is the main method in current carbon dioxide capture technology. For the gas separation, there are four main processes: Absorption, Cryogenic Separation, Membrane Separation, and Adsorption. Wang et al. (2013) compared different procedures, and the result has shown that the energy consumption of the adsorption method is better than the absorption method. Patil et al. (2018) used AMP/PZ/water mixture in a close-loop adsorber-desorber system to separate the $CO_2$ from post-combustion gas ($CO_2$-$N_2$ mixture, $CO_2$ 12 mol %), resulting in 85 % removability and energy consumption is 3.78 MJ/kg$CO_2$. Shen et al. (2012) used activated carbon in a two-stage vacuum pressure swing adsorption process to separate flue gas of 15 % $CO_2$ as feed. The best experimental results can obtain 94.14 % $CO_2$ purity with 85.08 % recovery, productivity $1.139 \cdot 10^{-3}$ mol/kg-s, and the best simulation results were 96.34 % $CO_2$ purity with 80.72 % recovery, productivity $2.58 \cdot 10^{-4}$ mol/kg-s, and 829.28 kJ/kg-$CO_2$ energy consumption. Wang et al. (2012) simulated a modified two-stage vacuum pressure swing adsorption program to capture carbon dioxide in the flue gas of 15 % $CO_2$. The first stage used a 3-bed 5-step process, and the second stage uses a 2-bed

Paper Received: 27/03/2020; Revised: 01/06/2020; Accepted: 07/06/2020
Please cite this article as: Cheng C.-Y., Kuo C.-C., Yang M.-W., Zhuang Z.-Y., Lin P.-W., Yang H.-S., Chou C.-T., 2020, Simulation of Carbon Capture from Flue Gas of a Coal-fired Power Plant by a Three-bed Pressure Swing Adsorption Process, Chemical Engineering Transactions, 81, 415-420 DOI:10.3303/CET2081070

6-step process. Both used zeolite 13X-APG as adsorbent and the results showed that 96.54 % $CO_2$ purity with 93.35 % recovery, energy consumption 528.39 kJ/kg$CO_2$, and productivity $8.61 \cdot 10^{-6}$ kg$CO_2$/kg-s were obtained. This study used EIKME 13X zeolite as the adsorbent and 13.5 % carbon dioxide balanced by nitrogen as feed. The feed flow rate of 1 kW coal-fired power plants referred to the National Energy Technology Laboratory (NETL) report (2015). In order to find the optimal operating conditions, this study used the central composite design for analysis. Before this study, there was no PSA process used for carbon capture in Taiwan's power plant. The goal of this study is to develop a PSA process to capture $CO_2$ for 1 kW flue gas in a coal-fired power plant of Taiwan Power Company, and the PSA process based on this paper is now operating at Taichung Power Plant.

## 2. Methodology

### 2.1 Mathematical modeling

The assumptions made for mathematical modeling, the corresponding equations and boundary conditions are mentioned in Chou et al. (2013). The linear driving force model and extended Langmuir-Freundlich isotherm are used in the simulation.
Extended Langmuir-Freundlich isotherm equation:

$$q_i^* = \frac{n_i^*}{\rho_s} = \frac{q_{m,i}\, b_i y_i^{m_i} P^{m_i}}{1 + \sum_{i=1}^{n} b_i y_i^{m_i} P^{m_i}} \tag{1}$$

where

$$q_{m,i} = a_{i,1} + (a_{i,2} T),\ b_i = b_{i,0} + exp(b_{i,1}/T),\ m_i = m_{i,1} + m_{i,2}/T \tag{2}$$

In Eq(1), $q_i$* represents the equilibrium adsorption amount of component i per unit adsorbent mass, $n_i^*$ represents the equilibrium adsorption amount of component i per unit adsorbent volume, $\rho_s$ is the density of the adsorbent, $P$ is pressure, $y_i$ is the mole fraction of component i and $T$ is temperature. The parameters used in Eq(2) are all isotherm parameters.
Linear driving force model:

$$\frac{\partial n_i}{\partial t} = k_{LDF,i}(n_i^* - n_i) \tag{3}$$

In Eq(3), $n_i$ represents the adsorption amount of component i per unit adsorbent volume.

### 2.2 PSA process

In this study, a 3-bed 9-step PSA process shown in Figure 1 was studied to capture $CO_2$ by simulation, the process is described as follows: Adsorption (AD), Pressure Equalisation (PE), Cocurrent Depressursation (CD), Vacuum (VA) and Idle (ID), and EIKME 13X was used as the adsorbent. The feed composition of the process referred to Wawrzyńczak et al. (2019). The flue gas emitted by the power plant is first desulfurised, then removed the water resulting in 13.5 % carbon dioxide and 86.5 % nitrogen. The goal is to obtain higher than 85 % purity of carbon dioxide and 90 % purity of nitrogen in two different streams.
In order to confirm the correctness of the parameters used in the program simulation, 100 h experimental data from a 3-bed 9-step 1 kW scale coal-fired power plant were used for verification.
The procedure of the process is shown in Figure 1. The step time and the parameters of the bed are shown in Tables 1 and Table 2.

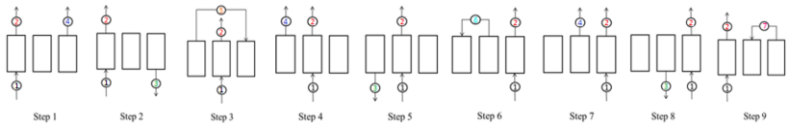


*Figure 1: Procedure of the 3-bed 9-step PSA process*

*Table 1: Step time of 3-bed 9-step PSA process*

| Step | 1 | 2 | 3 | 4 | 5 | 6 | 7 | 8 | 9 |
|---|---|---|---|---|---|---|---|---|---|
| Process | AD | AD | PE | CD | VA | PE | ID | ID | AD |
| Time (s) | 80 | 300 | 50 | 80 | 300 | 50 | 80 | 300 | 50 |

*Table 2: Parameters of the adsorption bed*

| Parameter | Value |
|---|---|
| Feed flow rate ($m^3$/s, NTP) | $10^{-3}$ |
| Bed length (m) | 0.4 |
| Bed diameter (m) | 0.16 |
| Feed temperature (K) | 303.14 |
| Feed pressure (atm) | 3 |
| Vacuum pressure (atm) | 0.07 |
| Cocurrent depressurisation pressure (atm) | 0.25 |

## 3. Results and discussion

### 3.1 Adsorption isotherms

The $CO_2$ and $N_2$ adsorption amount on EIKME 13X zeolite were measured by a micro-balance Thermo D-200. Langmuir-Freundlich isotherm, shown in Eq(1), was used as the equilibrium adsorption model and the parameters were fitted by The MATLAB Curve Fitting Toolbox and all parameters are shown in Table 3. The isotherm curves are shown in Figure 2 in which the error bars of 95 % confidence intervals are also shown.

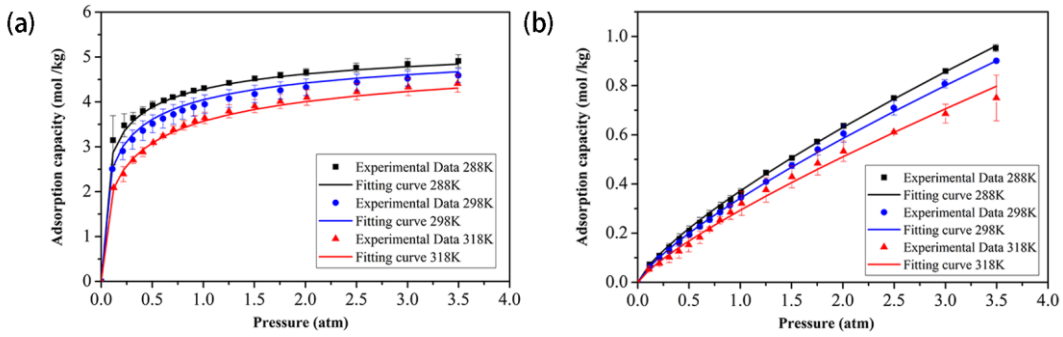


*Figure 2: Adsorption isotherm of (a) $CO_2$ and (b) $N_2$ on EIKME 13X zeolite*

*Table 3: Langmuir-Freundlich isotherm parameters of $CO_2$ and $N_2$ on zeolite 13X*

| | Carbon dioxide | Nitrogen |
|---|---|---|
| $a_{i,1}$(mole/kg) | 6.507 | $1.185 \cdot 10^{3}$ |
| $a_{i,2}$(mole/K·kg) | $-3 \cdot 10^{-3}$ | $-1.022 \cdot 10^{-1}$ |
| $b_{i,0}$(1/atm) | $8 \cdot 10^{-3}$ | $4.842 \cdot 10^{-4}$ |
| $b_{i,1}$(K) | $1.722 \cdot 10^{3}$ | $6.215 \cdot 10^{2}$ |
| $m_{i,1}$(-) | $6.013 \cdot 10^{-1}$ | 1.182 |
| $m_{i,2}$(K) | $-2.4 \cdot 10^{1}$ | $-1.2 \cdot 10^{2}$ |

### 3.2 Breakthrough curve and desorption curve verification

To verify the reliability of the linear driving force coefficient and the simulation program, a breakthrough curve experiment was performed. Figure 3 shows that the result of simulation can fit the experimental data of breakthrough curve and desorption curve. The operating conditions are shown in Table 4.

*Table 4: Operating parameters of breakthrough curve and desorption curve*

| | Breakthrough experiment | Desorption experiment |
|---|---|---|
| Feed composition | 15.0 % $CO_2$ | Pure He |
| Bed length (m) | 1 | 1 |
| Bed diameter (m) | $2.32 \cdot 10^{-2}$ | $2.32 \cdot 10^{-2}$ |
| Bed volume (L) | 0.42273 | 0.42273 |
| Feed pressure (atm) | 2.5 | 2.5 |
| Feed temperature (K) | 298 | 298 |
| Surrounding temperature (K) | 298 | 298 |
| Feed flow rate ($m^3$/s) | $1.67 \cdot 10^{-5}$ | $1.00 \cdot 10^{-5}$ |

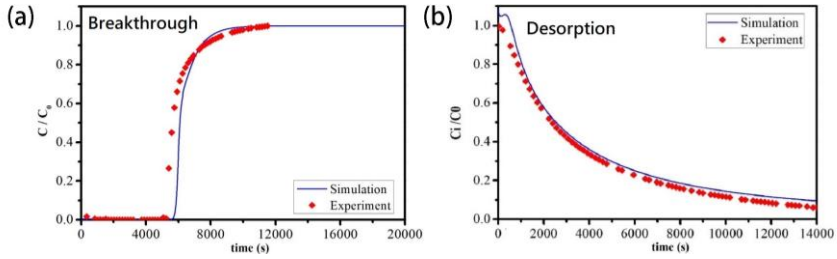


*Figure 3: Simulation of (a) breakthrough curve and (b) desorption curves*

### 3.3 3-bed 9-step PSA process verification

In this section, the average experimental data of the last 40 cycles of the 3-bed 9-step 100-hour cyclic-steady-state experiment are used for simulation verification. The cyclic-steady-state feed concentration of $CO_2$ is 15.36 % and concentration of $N_2$ is 84.64 %, the feed flow rate is $9.703 \cdot 10^{-4}$ $m^3/s$, the feed pressure is 3 atm, the vacuum pressure is 0.07 atm, the vent pressure is 0.25 atm, the surrounding temperature is 303.14 K and the feed temperature is 303.14 K.

*Table 5: Results of the 3-bed 9-step PSA process*

| Variables | Experiment | Simulation |
|---|---|---|
| Top vent flow rate ($m^3/s$, NTP) | $4.77 \cdot 10^{-5}$ | $7.03 \cdot 10^{-5}$ |
| $CO_2$ Purity/ Recovery (%) | 12.23/3.91 | 29.12/13.75 |
| $N_2$ Purity/ Recovery (%) | - | 70.88/6.08 |
| Bottom product flow rate ($m^3/s$, NTP) | $8.92 \cdot 10^{-5}$ | $8.92 \cdot 10^{-5}$ |
| $CO_2$ Purity/ Recovery (%) | 91.70/54.83 | 91.69/54.81 |
| $N_2$ Purity/ Recovery (%) | - | 8.31/0.90 |
| Top product flow rate ($m^3/s$, NTP) | $8.05 \cdot 10^{-4}$ | $8.11 \cdot 10^{-4}$ |
| $CO_2$ Purity/ Recovery (%) | 5.79/31.26 | 5.78/31.43 |

### 3.4 3-bed 9-step PSA process optimisation

The central composite design was used to determine the optimal result. Variables are as below: feed pressure, vacuum pressure, co-current depressurisation pressure, ambient temperature, time of co-current depressurisation step, time of vacuum step, and tower length. The effects of these seven variables on the purity and recovery of carbon dioxide at the bottom product and energy consumption were discussed. Finally, regression analysis was used to find the optimal response and optimal operating conditions. The high- , basic- and low-level setting values of each factor are shown in Table 6. Eq(4), Eq(5), and Eq(6) are the regression equations for bottom product $CO_2$ purity, bottom product $CO_2$ recovery, and energy consumption, which can be used for optimisation. In Figure 4, the red line indicated the optimal results of the seven variables. The optimisation results using the setting value from Figure 4 are shown in Table 7 and Table 8.

*Table 6: Operating parameter*

| Variables | - | 0 | + |
|---|---|---|---|
| A: Feed pressure (atm) | 2.0 | 3.0 | 4.0 |
| B: Vacuum pressure (atm) | 0.05 | 0.075 | 0.1 |
| C: Vent pressure (atm) | 0.2 | 0.3 | 0.4 |
| D: Surrounding temperature (K) | 288.14 | 305.64 | 323.14 |
| E: Step 1/4/7 (Cocurrent depressurisation) time (s) | 40 | 80 | 120 |
| F: Step 2/5/8 (vacuum) time (s) | 250 | 300 | 350 |
| G: Bed length (m) | 0.3 | 0.4 | 0.5 |

$$\begin{aligned} Purity\ (\%) = {} & 208.683 + 8.44694\ (1/atm)\ A - 136.4\ (1/atm)\ B - 10.6067\ (1/atm)\ C - 1.03797\ (1/K)\ D + 0.254009\ (1/s)\ E + \\ & 0.0168206\ (1/s)\ F + 0.753353\ (1/cm)\ G - 1.11434\ (1/atm^2)\ A \cdot A + 303.611\ (1/atm^2)\ B \cdot B - 14.7843\ (1/atm^3)\ C \cdot C + \\ & 0.00176753\ (1/K^2)\ D \cdot D - 0.00158675\ (1/s^2)\ E \cdot E + 0.0001\ (1/s^2)\ F \cdot F + 0.000643\ (1/cm^2)\ G \cdot G - 0.31307\ (1/atm^2)\ A \cdot B + \\ & 12.9433\ (1/atm^2)\ A \cdot C + 0.000388\ (1/atm \cdot K)\ A \cdot D + 0.015792\ (1/atm \cdot s)\ A \cdot E + 0.00384\ (1/atm \cdot s)\ A \cdot F - \\ & 0.08853\ (1/atm \cdot cm)\ A \cdot G - 45.2696\ (1/atm^2)\ B \cdot C + 0.436755\ (1/atm \cdot K)\ B \cdot D + 0.499657\ (1/atm \cdot s)\ B \cdot E - \\ & 0.239613\ (1/atm \cdot s)\ B \cdot F - 0.862748\ (1/atm \cdot cm)\ B \cdot G - 0.0234598\ (1/atm \cdot K)\ C \cdot D - 0.323612\ (1/atm \cdot s)\ C \cdot E - \\ & 0.0206273\ (1/atm \cdot s)\ C \cdot F + 0.103386\ (1/atm \cdot cm)\ C \cdot G + 0.0004568\ (1/K \cdot s)\ D \cdot E - 4.61 \cdot 10^{-5}\ (1/K \cdot s)\ D \cdot F - \\ & 0.00292673\ (1/K \cdot cm)\ D \cdot G - 1.59 \cdot 10^{-4}\ (1/s^2)\ E \cdot F + 0.00148013\ (1/s \cdot cm)\ E \cdot G - 2.7 \cdot 10^{-4}\ (1/s \cdot cm)\ F \cdot G \end{aligned} \quad (4)$$

$$Recovery\ (\%) = -54.8248 + 5.70294\ (1/atm)\ A - 290.665\ (1/atm)\ B - 1.79674\ (1/atm)\ C + 0.949833\ (1/K)\ D - 0.100019\ (1/s)\ E - 0.0570018\ (1/s)\ F - 1.02886\ (1/cm)\ G - 1.816\ (1/atm^2)\ A \cdot A - 1406.76\ (1/atm^2)\ B \cdot B - 29.2673\ (1/atm^2)\ C \cdot C - 0.0016378\ (1/K^2)\ D \cdot D - 1.65144 \cdot 10^{-5}\ (1/s^2)\ E \cdot E - 2.19 \cdot 10^{-4}\ (1/s^2)\ F \cdot F - 0.0115602\ (1/cm^2)\ G \cdot G + 95.1987\ (1/atm^2)\ A \cdot B - 4.91901\ (1/atm^2)\ A \cdot C - 0.001048\ (1/atm \cdot K)\ A \cdot D - 0.0285889\ (1/atm \cdot s)\ A \cdot E - 0.00544839\ (1/atm \cdot s)\ A \cdot F + 0.186206\ (1/atm \cdot cm)\ A \cdot G + 163.14\ (1/atm^2)\ B \cdot C - 0.403525\ (1/atm \cdot K)\ B \cdot D - 0.9026\ (1/atm \cdot s)\ B \cdot E - 0.269244\ (1/atm \cdot s)\ B \cdot F + 3.48384\ (1/atm \cdot cm)\ B \cdot G - 0.0252969\ (1/atm \cdot K)\ C \cdot D + 0.240571\ (1/atm \cdot s)\ C \cdot E + 0.0666479\ (1/atm \cdot s)\ C \cdot F + 0.135799\ (1/atm \cdot cm)\ C \cdot G + 7.99 \cdot 10^{-5}\ (1/K \cdot s)\ D \cdot E + 1.60842 \cdot 10^{-4}\ (1/K \cdot s)\ D \cdot F + 0.00265063\ (1/K \cdot cm)\ D \cdot G - 1.21 \cdot 10^{-4}\ (1/s^2)\ E \cdot F + 0.0029009\ (1/s \cdot cm)\ E \cdot G + 0.0012076\ (1/s \cdot cm)\ F \cdot G \quad (5)$$

$$Energy\ consumption\ (GJ/t - CO_2) = 1.1382 + 0.714472\ (1/atm)\ A + 1.09506\ (1/atm)\ B + 0.448582\ (1/atm)\ C - 0.0099\ (1/K)\ D + 0.00436957\ (1/s)\ E - 0.00259758\ (1/s)\ F + 0.0097060\ (1/cm)\ G - 0.038474\ (1/atm^2)\ A \cdot A + 36.4096\ (1/atm^2)\ B \cdot B + 0.0355262\ (1/atm^2)\ C \cdot C + 1.85 \cdot 10^{-5}\ (1/K^2)\ D \cdot D + 6.29 \cdot 10^{-6}\ (1/s^2)\ E \cdot E + 6.12 \cdot 10^{-6}\ (1/s^2)\ F \cdot F + 1.85442 \cdot 10^{-4}\ (1/cm^2)\ G \cdot G - 0.0859038\ (1/atm^2)\ A \cdot B - 0.00750255\ (1/atm^2)\ A \cdot C - 2.83 \cdot 10^{-4}\ (1/atm \cdot K)\ A \cdot D + 0.00132517\ (1/atm \cdot s)\ A \cdot E - 2.33 \cdot 10^{-4}\ (1/atm \cdot s)\ A \cdot F - 0.00373936\ (1/atm \cdot cm)\ A \cdot G - 4.36119\ (1/atm^2)\ B \cdot C - 0.00479232\ (1/atm \cdot K)\ B \cdot D + 0.032285\ (1/atm \cdot s)\ B \cdot E + 0.0011352\ (1/atm \cdot s)\ B \cdot F - 0.08924\ (1/atm \cdot cm)\ B \cdot G + 7.96313 \cdot 10^{-4}\ (1/atm \cdot K)\ C \cdot D - 0.005784\ (1/atm \cdot s)\ C \cdot E - 1.21 \cdot 10^{-4}\ (1/atm \cdot s)\ C \cdot F + 0.00448796\ (1/atm \cdot cm)\ C \cdot G - 5.44 \cdot 10^{-6}\ (1/K \cdot s)\ D \cdot E - 1.27 \cdot 10^{-6}\ (1/K \cdot s)\ D \cdot F - 1.23 \cdot 10^{-5}\ (1/K \cdot cm)\ D \cdot G - 7.19 \cdot 10^{-6}\ (1/s^2)\ E \cdot F - 6.56 \cdot 10^{-5}\ (1/s \cdot cm)\ E \cdot G - 1.20 \cdot 10^{-5}\ (1/s \cdot cm)\ F \cdot G \quad (6)$$

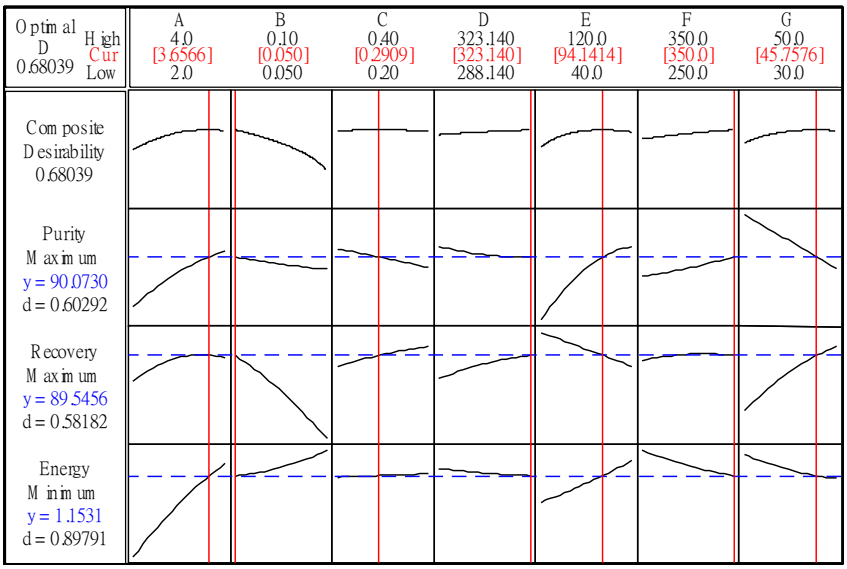


*Figure 4: The optimal response of regression from purity, recovery and energy consumption*

*Table 7: Optimal operating condition of capturing $CO_2$ from flue gas by PSA process*

| Parameter | Value |
|---|---|
| Feed composition | 13.5 % $CO_2$, 86.5 % $N_2$ |
| Feed flow rate ($m^3/s$, NTP) | $1.21 \cdot 10^{-3}$ |
| Bed length (m) | 0.46 |
| Bed inner diameter (m) | 0.16 |
| Bed volume (L) | 9.2488 |
| Bed porosity (-) | 0.6937 |
| Fluid viscosity (kg/m-s) | $1.87 \cdot 10^{-5}$ |
| Overall heat transfer coefficient ($J/m^2 \cdot s \cdot K$) | 10.8 |
| Feed temperature (K) | 303.14 |
| Surrounding temperature (K) | 323.14 |
| Feed pressure (atm) | 3.66 |
| Vacuum pressure (atm) | 0.05 |
| Cocurrent depressurisation pressure (atm) | 0.3 |
| Step time (s) | 94, 350, 50, 94, 350, 50, 94, 350, 50 |

*Table 8: The results of simulation before and after central composite design analysis from purity, recovery and energy consumption*

| Variables | Simulation for basic case | Prediction from Regression | Simulation after CCD |
|---|---|---|---|
| Purity (%) | 85.96 | 89.83 | 89.20 |
| Recovery (%) | 82.09 | 89.78 | 88.20 |
| Energy consumption (GJ/t) | 1.06 | 1.15 | 1.17 |

## 4. Conclusions

In this study, the isotherm parameters were obtained by fitting the $CO_2$ and $N_2$ adsorption data from the experiment. The breakthrough curve and desorption experiments performed at the lab-scale were used to verify the simulation accuracy. The agreement is good. The 3-bed 9-step experimental process was used to capture the flue gas from the power plant for the 100 h cyclic-steady-state experiment. The average composition of the feed gas is 15.36 % carbon dioxide and 84.64 % nitrogen for the last 40 cycles of the 100-hour PSA experiment. The comparison between the experiments and simulation show that the simulation result is reliable. Finally, this study used the central composite design (CCD) and regression analysis to find the optimal purity, recovery, and minimum energy consumption with 13.5 % carbon dioxide 86.5 % nitrogen feed composition. The result showed that the purity of the carbon dioxide in the bottom product can reach 89.20 % with a recovery 88.20 %, and the purity of the nitrogen in the top product can reach 98.49 % with a recovery 93.56 %, and the power consumption was 1.17 - 1.41 GJ/t-$CO_2$ under optimal conditions: feed pressure = 3.66 atm, vacuum pressure = 0.05 atm, co-current depressurisation pressure = 0.3 atm, surrounding temperature = 323.14 K, step 1/4/7 time = 94 s, step 2/5/8 time = 350 s and tower length = 0.46 m.

**Acknowledgements**

The authors wish to thank the Taiwan Power Company for financial support.

## References

Chou C., Chen F., Huang Y., Yang H., 2013, Carbon dioxide capture and hydrogen purification from synthesis gas by pressure swing adsorption, Chemical Engineering Transactions, 32, 1855 - 1860.

Le Quéré C., Andrew R.M., Friedlingstein P., Sitch S., Hauck J., Pongratz J., Pickers P.A., Korsbakken J.I., Peters G. P., Canadell J.G., Arneth A., Arora V.K., Barbero L., Bastos A., Bopp, L., Chevallier F., Chini L. P., Ciais P., Doney S.C., Gkritzalis T., Goll D.S., Harris I., Haverd V., Hoffman F. M., Hoppema M., Houghton R.A., Hurtt G., Ilyina T., Jain A.K., Johannessen T., Jones C.D., Kato E., Keeling R.F., Goldewijk K.K., Landschützer P., Lefèvre N., Lienert S., Liu Z., Lombardozzi D., Metzl N., Munro D.R., Nabel J.E.M.S., Nakaoka S., Neill C., Olsen A., Ono T., Patra P., Peregon A., Peters W., Peylin P., Pfeil B., Pierrot D., Poulter B., Rehder G., Resplandy L., Robertson E., Rocher M., Rödenbeck C., Schuster U., Schwinger J., Séférian R., Skjelvan I., Steinhoff T., Sutton A., Tans P.P., Tian H., Tilbrook B., Tubiello F. N., van der Laan-Luijkx I.T., van der Werf G.R., Viovy N., Walker A.P., Wiltshire A.J., Wright R., Zaehle S., Zheng B., 2018, Global carbon budget 2018, Earth System Science Data, 10, 2141 – 2194.

National Energy Technology Laboratory, 2015, Cost and Performance Baseline for Fossil Energy Plants, The United State Department of Energy, 1a, rev. 3.

Patil M., Vaidya P., Kenig E., 2018, Bench-scale study for $CO_2$ capture using AMP/PZ/water mixtures, Chemical Engineering Transactions, 69, 163 - 168.

Shen C.Z., Liu Z., Li P., Yu J.G., 2012, Two-stage VPSA process for $CO_2$ capture from flue gas using activated carbon beads, Industrial & Engineering Chemistry Research, 51, 5011 - 5021.

Wang L., Liu Z., Li P., Wang J., Yu J.G., 2012, $CO_2$ capture from flue gas by two successive VPSA units using 13XAPG, Adsorption Journal of the International Adsorption Society, 18, 445 – 459.

Wang L., Yang Y., Shen W., Kong X., Li P., Yu J., Rodrigues A.E., 2013, $CO_2$ capture from flue gas in an existing coal-fired power plant by two successive pilot-scale VPSA units, Industrial & Engineering Chemistry Research, 52, 7947 – 7955.

Wawrzynczak D., Majchrzak-Kuceba I., Srokosz K., Kozak M., Nowak W., Zdeb J., Smolka W., Zajchowski A., 2019, The pilot dual-reflux vacuum pressure swing adsorption unit for $CO_2$ capture from flue gas, Separation and Purification Technology, 209, 560 – 570.